Special Issue Article

Phytochemical Analysis

Received: 23 January 2013, Revised: 8 May 2013, Accepted: 13 May 2013 Published online in Wiley Online Library: 24 June 2013

(wileyonlinelibrary.com) DOI 10.1002/pca.2456

Stability and Oxidation Products of Hydrolysable Tannins in Basic Conditions Detected by HPLC/DAD–ESI/QTOF/MS

Anu Tuominen* and Terhi Sundman

ABSTRACT:

Introduction – Hydrolysable tannins occur in plants that are used for food or medicine by humans or herbivores. Basic conditions can alter the structures of tannins, that is, the oxidation of phenolic groups can lead to the formation of toxic quinones. Previously, these labile quinones and other oxidation products have been studied with colorimetric or electron paramagnetic resonance methods, which give limited information about products.

Objective – To study the stability and oxidation products of hydrolysable tannins in basic conditions using HPLC with a diode-array detector (DAD) combined with electrospray ionisation (ESI) and quadrupole time-of-flight (QTOF) MS.

Methods – Three galloyl glucoses, four galloyl derivatives with different polyols and three ellagitannins were purified from plants. The incubation reactions of tannins were monitored by HPLC/DAD at five pH values and in reduced oxygen conditions. Reaction products were identified based on UV spectra and mass spectral fragmentation obtained with the high-resolution HPLC/DAD–ESI/QTOF/MS. The use of a base-resistant HPLC column enabled injections without the sample pre-treatment and thus detection of short-lived products.

Results – Hydrolysable tannins were unstable in basic conditions and half-lives were mostly less than 10 min at pH 10. Degradation rates were faster at pH 11 but slower at milder pH. The HPLC analyses revealed that various products were formed and identified to be the result of hydrolysis, deprotonation and oxidation. Interestingly, the main hydrolysis product was ellagic acid; it was also formed from galloyl glucoses that do not contain oxidatively coupled galloyl groups in their initial structures.

Conclusion – HPLD/DAD–ESI/QTOF/MS was an efficient method for the identification of polyphenol oxidation products and showed how different pH conditions determine the fate of hydrolysable tannins. Copyright © 2013 John Wiley & Sons, Ltd.

Keywords: HPLC/DAD–MS; hydrolysis; polyphenol oxidation; ellagitannins; galloyl glucoses; galloyl quinic acids; plant defence

Introduction

Hydrolysable tannins (HTs) are phenolic secondary metabolites that occur in many plant parts that are used as a food source for humans or herbivores. Hydrolysable tannins are considered to be the effective constituents in many plant-derived traditional medicines. Usually D-glucose is at the centre of the HT molecule, but other polyols such as quinic acid or shikimic acid also occur. Hydrolysable tannins can be divided into galloyl derivatives and ellagitannins (ETs). Ellagitannins are synthetised by plants from galloyl glucoses (GGs) by the oxidative coupling of galloyl groups to form a hexahydroxydiphenoyl (HHDP) group. A HHDP group can be further transformed through oxidation or coupling. As the name also describes the ester bonds of HTs are readily hydrolysed. Partial hydrolysis in the structure elucidation of HTs can be done with boiling water, tannase enzyme or weak acid (Yoshida *et al*., 1992). It has been traditionally thought that galloyl glucoses yield gallic acid as hydrolysis products and ETs yield ellagic acid (EA) or other similar products depending on the initial structure. Hydrolysable tannins are weakly acidic compounds and thus stable in acidic conditions and usually their HPLC analysis is performed with a mildly acidic buffer and from neutral sample solutions. The reactions of HTs in different basic solutions are not well studied and numeric data about their stability are rare. Typically, it has been reported that some browning and degradation occurs in basic conditions (Hemingway and Hillis, 1971; Barbehenn *et al*., 2006).

Hydrolysable tannins can precipitate proteins and form complexes with heavy metals. In plants, the protein precipitating capacity of HTs traditionally has been considered as a defensive function against herbivores and pathogens. However, the gut conditions of herbivores such as the pH level, oxygen level and redox conditions can affect the reactions of plant tannins (Johnson and Barbehenn, 2000; Gross *et al*., 2008). The gut conditions can transform or change the structure of tannins and thus activate their defensive functions and make them more toxic (Appel, 1993). For example, the hydrolysis products of HTs can be more harmful to herbivores because they might be absorbed more easily by insect tissues than initial tannins (Barbehenn and Constabel, 2011). Many Lepidoptera larvae, especially, have highly basic gut conditions (pH 9–12), which favour the auto-oxidation of tannins (Appel and Martin, 1990;

* Correspondence to: A. Tuominen, Laboratory of Organic Chemistry and Chemical Biology, Department of Chemistry, FI-20014 University of Turku, Finland. E-mail: ankatu@utu.fi

Laboratory of Organic Chemistry and Chemical Biology, Department of Chemistry, FI-20014 University of Turku, Finland

Appel, 1993; Gross *et al*., 2008; Salminen and Karonen, 2011). Tannin oxidation produces quinones that are highly reactive electrophilic molecules and generally more toxic substances than phenols. Quinones are possibly able to bind covalently with proteins or damage essential nutrients and produce reactive oxygen species that can cause oxidative stress on herbivores' tissues (Appel, 1993), although recent studies have not yet validated this hypothesis (Barbehenn *et al*., 2009, 2012).

The relatively stable oxidation products of polyphenols can be isolated for structure determination (e.g. Tanaka *et al*., 1990; Hatano *et al*., 2004). Also, some *in vitro* methods have been developed to measure the pro-oxidant capacity of tannins and to detect short-lived oxidation products such as radicals that cannot be isolated as pure compounds. In those studies, electron paramagnetic resonance spectroscopy has been used to detect the semiquinone radicals (Barbehenn *et al*., 2006), or a simple colorimetric method using one wavelength that measures the browning rate of the sample has been used in the evaluation of the maximum rate of oxidation of pure ETs at pH 10 (Moilanen and Salminen, 2008) or the pro-oxidant capacity of crude plant extracts (Salminen and Karonen, 2011). However, with those previously used methods individual products and product structures cannot be determined.

Therefore, in this work, we wanted to obtain more detailed data about the oxidation products of pure HTs using HPLC with a diode-array detector (DAD) combined with MS. *In vitro* conditions were broadened to include five pH values. Also, incubation in a reduced oxygen level was studied in order to better cover the full scale of the herbivory gut conditions that plant HTs might confront. Ten structurally distinct HTs were chosen for study, including three galloyl glucoses, four other galloyl derivatives with different polyols and three ETs. In addition to typical HT structures, study compounds were selected because of the high pro-oxidant activity of plant extracts reported in previous studies: geraniin and galloyl quinic acids of *Geranium sylvaticum* (Tuominen *et al*., unpublished), the galloyl derivatives of *Acer rubrum* (Barbehenn *et al*., 2008) and the epigallocatechin gallate of green tea (Elbling *et al*., 2005). The *in vitro* method and sample treatment were further developed to be as fast as possible in order to study the degradation rates and products that formed under alkaline conditions. Sample solutions were incubated in a well plate and reactions were monitored by HPLC/DAD as such without pre-treatments. The acidic mobile phase neutralised the sample on-line. This approach was possible with the use of a HPLC column that was robust with a large pH range. After these kinetic measurements by HPLC/DAD the various reaction products were identified with high-resolution HPLC/DAD combined with electrospray ionisation (ESI) and quadrupole time-of-flight (QTOF) MS based on their UV spectra and mass spectral fragmentations. This way we were able to evaluate the reactions of HTs based on the products that formed under different pH conditions and in the time scale.

Experimental

Extraction and isolation of HTs

Ten HTs were isolated from several plant materials (Table 1). The source of *Camellia sinensis* was commercial green tea (Twining & Company Ltd). *Acer rubrum* leaves were collected from Michigan, USA. *Betula pubenscens* and *Geranium sylvaticum* plant parts were collected from the Turku area, in southwest Finland. Dried plant powders were ground

Table 1. The details of hydrolysable tannins used in this study and reference for spectral data

Number	Compound	Source	Purity (HPLC–DAD) (%)	$b/10^{-3}$ (mM)	r^2	Reference
1	1-*O*-Galloyl-β-D-glucopyranose	*Geranium sylvaticum* roots	96	3.29	0.9994	Saijo *et al*., 1990
2	4-*O*-Galloyl quinic acid	*Geranium sylvaticum* roots	97	4.29	0.9945	Nishimura *et al*., 1984
3	(−)-Epigallocatechin-3-*O*-gallate	*Camellia sinensis* leaves	97	3.72	0.9989	Davis *et al*., 1996
4	1,6-Di-*O*-galloyl-β-D-glucopyranose	*Betula pubescens* leaves	97	1.67	0.9994	Salminen *et al*., 2001
5	4,5-Di-*O*-galloyl quinic acid	*Geranium sylvaticum* roots	86	2.08	0.9985	Nishimura *et al*., 1984
6	2,6-Di-*O*-galloyl-1,5-anhydro-D-glucitol	*Acer rubrum* leaves	100	1.83	0.9997	Hatano *et al*., 1990
7	1,2,3,4,6-Penta-*O*-galloyl-β-D-glucopyranose	Synthetised from tannic acid	99	0.70	0.9989	Saijo *et al*., 1990
8	1,2-Digalloyl-4,6-HHDP-β-D-glucopyranose	*Geranium sylvaticum* roots	93	1.37	0.9967	Yagi *et al*., 2009
9	Pedunculagin	*Betula pubescens* leaves	97	2.41	0.9995	Salminen *et al*., 2001
10	Geraniin	*Geranium sylvaticum* leaves	94	2.12	0.9994	Haddock *et al*., 1982
11	Ellagic acid	Sigma	95	0.57	0.9999	

b is the standard curve slope value at λ 280 nm (except λ 252 nm for **11**) used in the quantification of peak areas.

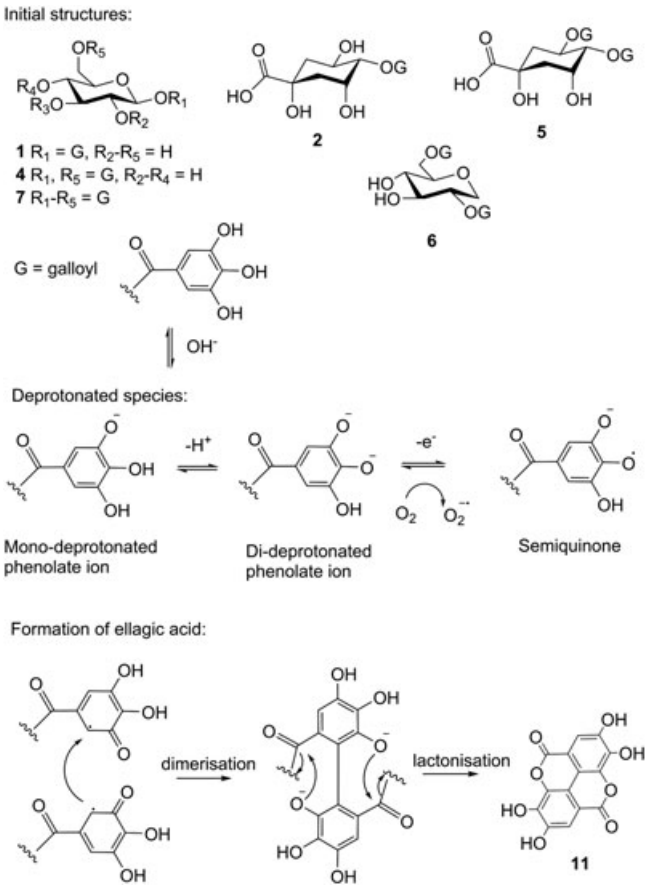

Figure 1. Structures of galloyl derivatives used in this study and their proposed reactions in basic conditions. The compound numbers refer to Table 3.

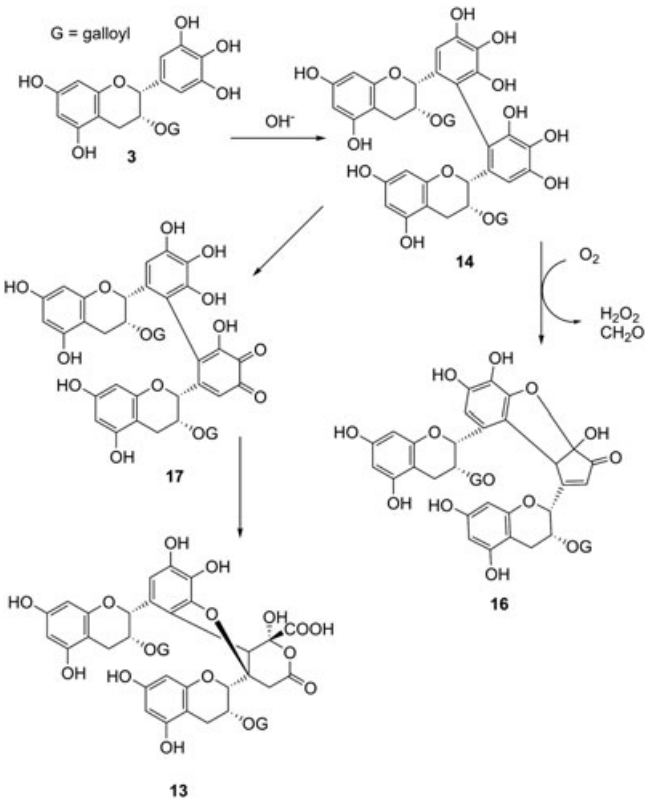

Figure 2. Detected reaction products of epigallocatechin gallate in basic conditions. The compound numbers refer to Table 3.

and extracted three times with large amounts of acetone:water (7:3, v/v) with a planary shaker. A 10 g amount of freeze-dried extract was dissolved in a small volume of water and applied to a Sephadex LH-20 column. Several fractions were collected by elution with water, and aqueous mixtures of methanol and acetone. The fractions obtained were concentrated into the aqueous phase by rotary evaporation and then freeze-dried. The purification of individual compounds from suitable Sephadex LH-20 fractions was performed by preparative HPLC with a Merck Li-Chroprep RP-18 (440 × 37.0 mm i.d., 40–63 μm) column (Merck, Darmstadt, Germany) and a semi-preparative Phenomenex Gemini RP-18 (150 × 21.20 mm i.d., 10 μm) column (Phenomenex, Torrance, CA, USA). The preparative HPLC system was from Waters (Milford, MA, USA) and it consisted of a Delta 600 pump, 2998 DAD detector, 600 controller, fraction collector III and Masslynx V4.1 management system. Elutions were performed with varying gradients of methanol:water (0:100 → 80:20, *v/v*) and 10 mL fractions were collected with Waters fraction collector. The fractions obtained were concentrated into the aqueous phase by rotary evaporation and then freeze-dried. The chemical structures of isolated HTs were characterised on the basis of their UV, mass and NMR spectra. All NMR spectra were measured with a Bruker Avance 500 spectrometer (Fällanden, Switzerland).

The degradation of initial compounds was quantified from the peak areas in the HPLC chromatograms against external standard curves. Standard solutions of HTs were prepared in water and 10–50% of ethanol was used to ease the dissolution. The concentration of HT solutions was 2.4 mM, except for **7**, **8** and **10** (Table 1) where it was only 1.5 mM because of their stronger absorption at the detection wavelength 280 nm. Ellagic acid (Sigma, Steinheim, Germany) has a poor water-solubility and therefore a small amount of pH 10 buffer was added to its solution before water. This resulted in a clear, greenish yellow, ellagic acid aqueous solution.

Incubation of HTs in buffers

Five commercially available Dilut-it buffers (J.T. Baker, Deventer, Holland) were used in the incubation of HTs: pH 3 (citric acid/sodium hydroxide/sodium chloride), pH 8 (sodium borate decahydrate), pH 9 (hydrochloric acid/sodium borate decahydrate), pH 10 (sodium carbonate/sodium bicarbonate) and pH 11 (sodium hydroxide/potassium chloride/boric acid). Compounds **2**, **3**, **5** and **6** (Table 1) were studied only at pH 10 and other HTs in all five buffers. Incubation at reduced oxygen level was studied for compounds **7** and **8**. The oxygen level of buffers was decreased by sparging with nitrogen for at least 15 min using a magnetic stirrer just before use. Also air was replaced with nitrogen before the sealing of the reaction well. The effectiveness of oxygen removal by sparging with nitrogen was measured with the Winkler method (Winkler, 1888). The initial oxygen level of ultrahigh-quality water used in the effectiveness test was 7.41 ± 0.03 mg/L. The sample treatment was developed to be as fast as possible. Buffers and samples were filtered through polytetrafluoroethylene (PTFE) 0.45 μm filters before mixing them together. Incubations were carried out in a 96-well plate, which was sealed with plastic to prevent evaporation at room temperature of 22 ± 1°C. The ratio of HT solution to buffer was 1:9 in a reaction well. Samples were injected straight from the sealed well plate. The incubations of HTs were followed for at least 4 h to a maximum of 6 h with 1 h injection intervals. More frequent analysis intervals (2, 20 and 40 min) were used in the beginning of the incubation at higher pH values for those HTs that degraded fast. Assays were performed in triplicate.

HPLC/DAD–MS analysis

The incubations of HTs were monitored with HPLC/DAD and reaction products were identified with HPLC–ESI/QTOF/MS. Reaction monitoring was performed with an Ultimate 3000 Series HPLC/DAD system (Dionex Corporation, Sunnyvale, CA, USA) consisting of an LPG-3400A pump, a WPS-3000SL autosampler and a PDA-3000 detector. The chromatographic management system was Chromeleon version 6.80 (Dionex Corporation, Sunnyvale, CA, USA). The analyses were done using the XBridge™ C_{18}-column (100 mm × 2.1 mm i.d., 3.5 mm) from Waters (Milford, MA, USA) that has a wide pH range of 1–12. The mobile phase consisted of (A) 0.1% formic acid and (B) acetonitrile. The linear gradient programme was as follows: 0–28 min, 0–20% B in A; 28–34 min, 20–70% B in A. The flow rate was maintained at 0.3 mL/min. The injection volume was 10 mL. The fixed detection wavelength was mostly 280 nm, however, 252 nm was used for the quantification of ellagic acid. The UV spectra of compounds were recorded in the wavelength range 195–600 nm.

Reaction products were identified using HPLC/DAD–ESI/QTOF/MS. Representative samples of the reaction products were prepared by mixing the buffer and the HT solution in a ratio 1:1. An Agilent 1200 Series HPLC system (Agilent Technologies, Waldbronn, Germany) consisted of a binary pump, a Hip-ALS SL autosampler, a DAD SL detector and a control module. The HPLC system was controlled by Hystar software version 3.2. (Bruker BioSpin, Rheinstetten, Germany). Chromatographic conditions were otherwise similar to those used in the reaction monitoring by HPLC/DAD. The HPLC system was connected to a Bruker micrOTOF-$_Q$ ESI hybrid quadrupole with a time-of-flight mass spectrometer (Bruker Daltonics, Bremen, Germany). The mass spectrometer was controlled by Compass micrOTOF control software (Bruker Daltonics) and operated in a negative ion mode. The capillary voltage was maintained at +4000 V with the end-plate offset at −500 V. The pressure for the nebuliser gas (N_2) was set at 1.6 bar and the drying gas (N_2) temperature at 200°C. The full scan mass ranged from *m/z* 50 up to 2000. Calibration with 5 mM sodium formate was used at the end of each sample in order to provide high-accuracy mass measurements. The data were handled by Compass DataAnalysis software (Version 4.0; Bruker Daltonics).

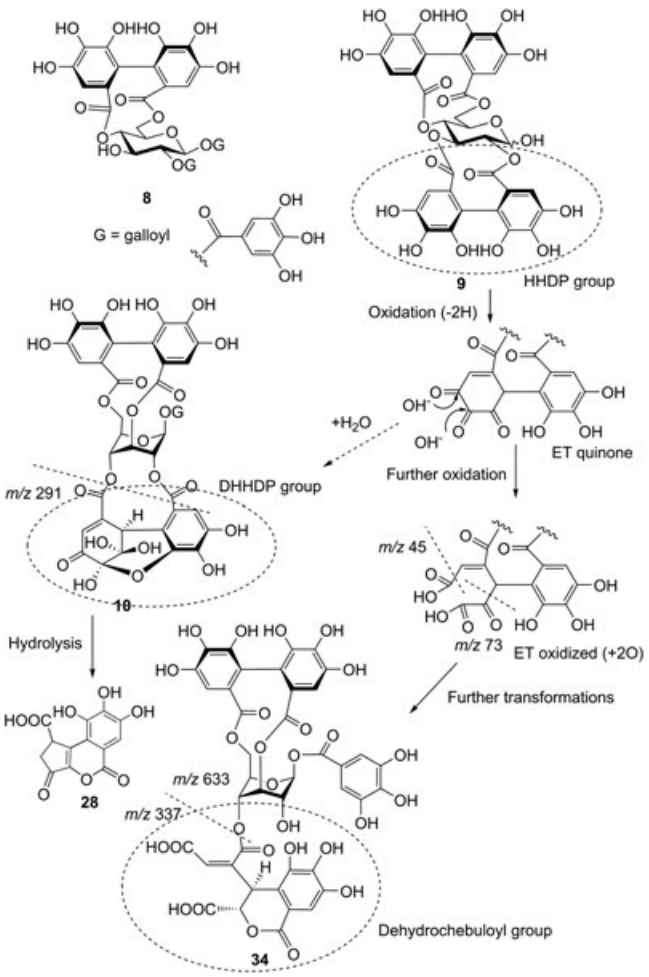

Figure 3. Structures of ellagitannins used in this study. Their proposed oxidation pathway is also presented. The compound numbers refer to Table 3.

Results and discussion

The purity of isolated HTs by HPLC and the standard curve values used are presented in Table 1. Structures of studied smaller galloyl derivatives **1**, **2** and **4–7** are presented in Fig. 1 except epigallocatechin gallate (EGCG, **3**; Fig. 2) and ellagitannins **8–10** (Fig. 3). The chromatograms of incubated HT solutions showed that the concentration of all HTs studied decreased in highly basic conditions (as an example the stability of ellagitannin **8** is shown in Fig. 4).

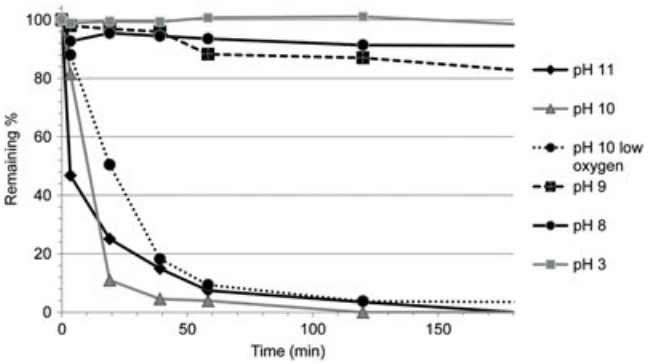

Figure 4. Stability of digalloyl-HHDP-glucose (**8**) at various pH values. Data are expressed as mean values of three samples.

Comparison of reaction kinetics

The degradation of HTs had different kinetics depending on alkalinity. The amount of HTs decreased exponentially at pH 10 and 11 and linearly at pH 9 and 8 (Fig. 4). At pH 3 all HTs studied were stable. The rate constants were calculated as first-order reactions so as to enable the comparison of the rate values (Table 2). In principle, degradation reactions were dependent only on the concentration of HT as there was an excess amount of buffer. The rate constant *k* was determined as the opposite of the slope of the plot $\ln([A]/[A]_0)$ versus reaction time (Table 2). Rate constants for all HTs could not be calculated at pH 8 and 9 because the degradation rate was too slow. The degradations at all pH values did not suitably fit the first-order curve and thus half-lives were estimated from degradation curves (Table 2, $t_{½curve}$).

The order of degradation rate achieved from rate constants and half-lives was slightly different. The reaction rates were first faster at pH 11 than at pH 10, but the concentration of the residual HTs was higher at pH 11 than at pH 10 after 20 min of incubation, as shown for ellagitannin **8** in Fig. 4. Therefore HTs were totally degraded at pH 10 in a shorter time than at pH 11

Table 2. The rate constants (k) and half-lives ($t_{½} \pm$ SE) for the degradation of hydrolysable tannins at 22°C, the maximum concentration of ellagic acid (EA) formed in the incubation and the time of formation at different pH values. Half-life $t_{½curve}$ is calculated from the equation of differently fitted degradation curves

	Number	pH	k (10^{-4} s^{-1})	r^2	$t_{½}$ curve (min)	c_{EAmax} (μM)	t_{EAmax} (h)	$c_{EAmax\ calc}$ (μM)	$c_{EAmax}/c_{EAmax\ calc}$ (%)
MonoGs	**1**	11	12.6 ± 1.4	0.9120	1.2 ± 0.1	31	1.4	120	25.8
		10	24.7 ± 1.3	0.9840	7.3 ± 0.8	73	0.7	120	60.8
		9	0.22 ± 0.01	0.9423	–	3.2	6[a]	120	2.7
		8	0.02 ± 0.01	0.5020	–	1.2	6[a]	120	1.0
	2	10	15.8 ± 1.0	0.9711	2.8 ± 0.2	55	1	120	45.8
	3	10	36.3 ± 1.8	0.9847	2.3 ± 0.1	2.1	6[a]	120	1.8
DiGs	**4**	11	14.0 ± 0.7	0.9705	2.0 ± 0.3	48	2	240	20.0
		10	25.5 ± 0.6	0.9972	6.2 ± 0.1	116	1	240	48.3
		9	0.18 ± 0.02	0.7948	–	4.9	6[a]	240	2.0
		8	0.02 ± 0.01	0.2769	–	2.2	6[a]	240	0.9
	5	10	11.1 ± 0.3	0.9956	15.5 ± 0.4	79	2	240	32.8
	6	10	26.9 ± 0.7	0.9962	4.1 ± 0.5	104	1	240	43.4
PentaG	**7**	11	1.7 ± 0.2	0.8832	240 ± 92	38	5	375	10.0
		10	7.7 ± 0.2	0.9932	22.7 ± 0.6	135	3	375	36.0
		10 low oxygen	3.5 ± 0.3	0.9208	50.1 ± 3.3	127	4[a]	375	33.9
		9	–		–	1.7	6[a]	375	0.5
		8	–		–	0.8	6[a]	375	0.2
ETs	**8**	11	6.2 ± 0.3	0.9841	1.7 ± 0.1	27	2	300	9.1
		10	18.6 ± 0.5	0.9926	7.7 ± 0.5	48	2	300	15.9
		10 low oxygen	8.4 ± 0.6	0.9277	24.6 ± 2.1	48	4[a]	300	15.8
		9	0.19 ± 0.01	0.9132	–	11	6[a]	300	3.8
		8	0.04 ± 0.01	0.7208	–	3.1	6[a]	300	1.0
	9	11	5.4 ± 0.9	0.7775	1.8 ± 0.2	82	1.5	480	17.1
		10	11.6 ± 0.7	0.9722	9.9 ± 0.8	19	2	480	4.0
		9	0.19 ± 0.01	0.9476	–	68	6[a]	480	14.2
		8	–		–	15	6[a]	480	3.0
	10	11	16.5 ± 1.0	0.9695	1.9 ± 0.2	3.6	2	225	1.6
		10	33.9 ± 0.7	0.9976	4.3 ± 0.4	12	1.5	225	5.1
		9	0.51 ± 0.01	0.9895	293 ± 43	2.3	6[a]	225	1.0
		8	0.09 ± 0.01	0.8730	–	1.2	6[a]	225	0.5

G, galloyl; ET, ellagitannins.
[a]Did not reach the maximum during analysis.

(Table 2). Rate constants at pH 8 and 9 did not differ substantially between HTs, except that geraniin (**10**) degraded faster than others. At pH 8 and at pH 9 over 90% and on average 70% of the HTs were left, respectively, after 6 h. Whereas, at pH 10 and 11, there were no initial compounds left after 1 h (Fig. 4 and Table 2). This substantial difference between pH 9 and 10 most likely results from the pK_a value of phenolic hydroxyl groups, which is approximately 9 (Appel, 1993). Thus the dissociation rate and the reactions of phenolic hydroxyl groups are more evident at pH above this.

Degradation was also dependent on compound structure, as already the HTs of the same size series had differences between rate constants at pH 10 (Table 2). Epigallocatechin gallate (**3**) yielded the highest rate constant of all the compounds studied (Table 2). Epigallocatechin gallate is the smallest tannin but not an HT because it is included in flavan-3-ol-based condensed tannins. However, its structure contains a galloyl group that is attached to the C ring of flavan-3-ol by an ester bond in the same way as the galloyl groups in HTs (Fig. 2).

PentaGG (**7**) was the most stable of the compounds studied in alkaline conditions and it was the only HT that reacted more slowly at pH 11 than at pH 10 (Table 2). Half-lives for all HTs were less than 10 min at pH 10 except for pentaGG (**7**) and **5**. PentaGG is the most hydrophobic galloyl glucose because it forms weak hydrophobic bond and hydrogen bond linkages between pentaGG molecules in water (Tanaka, 2009). These interactions might explain the low reactivity of **7** in basic conditions. Hydrogen bonds might shield the OH groups so that these are not easily deprotonated and might also protect some galloyl groups from hydrolysis since only 36% of possible EA is formed from **7** (Table 2). The oxidative coupling of galloyl groups makes ETs more water-soluble than **7** (Tanaka, 2009). Consequently, ETs degraded much faster than **7** (Table 2).

Dissolved oxygen in alkaline solutions can autoxidise tannins and produce tannin radicals. The level of oxygen in the purified water after 30 min sparging with nitrogen was 1.28 ± 0.11 mg/L, which means that a maximum of approximately 80% of oxygen was removed from the reagent solutions. However, this reduction in oxygen level already slowed down the degradation reactions significantly (Fig. 4 and Table 2.). The degradation of galloyl glucose **7** and ellagitannin **8** were both half slower in the reduced oxygen conditions. In spite of this, the end products

were the same as in the normal oxygen level and almost the same amount of EA was formed in reduced oxygen conditions but at the slower rate. Previously, the reduced oxygen conditions have similarly significantly slowed down the reactions of plant extract polyphenols at pH 8 (Gross *et al*., 2008).

Characterisation of degradation products

The direct injections from basic incubation media with short analysis time intervals allowed us to see the true variety of the degradation products of HTs in the HPLC chromatograms (Figs 5 and 6). The main degradation products were identified based on the characteristic UV spectra (Fig. 7 and Table 3) acquired with a DAD and the mass spectral data (Table 3) achieved with an accurate TOF mass spectrometer. The observed reaction products (Table 3) were divided into three groups: hydrolysis products, deprotonated species and other oxidatively transformed products. The structures of some potential degradation products are presented in Figs 1–3. Figure 8 presents the formation of degradation products in a time-scale for two representative compounds **4** and **9**.

Hydrolysis products. The primary reaction at pH values 8–10 was hydrolysis. Several smaller galloyl glucoses, such as **12**, **18** and **19** (Fig. 5D) formed after the cleavage of galloyl group (−152 Da), and ETs, such as **20** and **24** (Fig. 6), formed after the cleavage of the HHDP group (−302 Da), were observed as hydrolysis products (Table 3). Ellagic acid (**11**) is the typical hydrolysis product of ETs and it was detected as the main end product for almost all study compounds (for example Fig. 8). It was also the main product of monoG glucose (1) and monoG quinic acid (2), which do not contain HHDP groups in their initial structures (Fig. 1 and Fig. 5A). The amount of EA formed was smaller at pH 11 than at pH 10 for most of the HTs studied, thus it seems that pH 10 was the optimal pH level for EA formation (Table 2). Thus the hydrolysis rate explains the difference between the rate constants and the amounts that were left after 20 min of incubation at pH 10 and 11 (Fig. 4 and Table 2).

Deprotonated species. Several broad peaks that eluted before the initial compound were observed in the chromatograms of HTs incubated at higher pH values (**5d** in Fig. 5B, **8d** in Fig. 6B and **9d** in Fig. 6D). These products had UV and mass spectra similar to the initial compound and are therefore not listed in Table 3. These products were rationalised to be HTs containing deprotonated hydroxyl groups, that is, phenolate ions (Fig. 1), which explains their different retention behaviour in the column; phenolic compounds are weak acids that lose a proton when pH increases. When an analyte is ionised, it becomes less hydrophobic and, therefore, its retention decreases. However, the acidic mobile phase might reprotonate some of these deprotonated hydroxyl groups before the analyte reached the UV and MS detectors. Ellagitannin **9** has free hydroxyl in the glucose C-1 position and thus sugar transformations and formation of *C*-glycosidic ETs are also possible reactions of **9** (Tanaka *et al*., 1993).

The most intensive peaks of these deprotonated forms were of ETs **8** and **9** at pH 11 (Fig. 6B and D). For example, the deprotonated species of pedunculagin was at the highest concentration after 20 min at pH 10 and was totally depleted in 2 h (Fig. 8E). However, the number of peaks of deprotonated species differed between pH values and HTs (compare Fig. 6A with 6B and 6C with 6D). The multiple peaks in the HPLC–MS analysis may indicate that several hydroxyls were deprotonated when pH was higher than 10. Also, simple galloyl glucoses had several isomeric peaks in their chromatograms at all pH values (**1d** in Fig. 5A and **5d** in 5B) and the products decayed in a

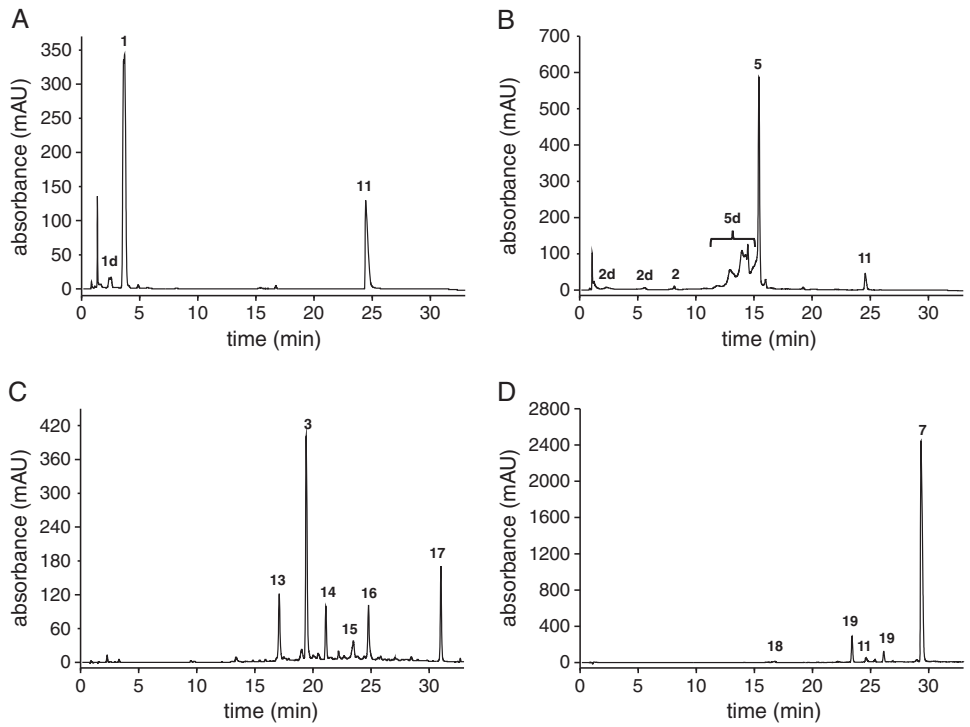

Figure 5. The HPLC chromatograms with detection wavelength 280 nm for galloyl derivatives at pH 10. (A) Monogalloyl glucose (**1**) after the incubation of 20 min; (B) digalloyl quinic acid (**5**) after incubation for 40 min; (C) epigallocatechin gallate (**3**) after the incubation of 20 min; (D) pentagalloyl glucose (**7**) after incubation for 1 h. The letter d indicates the deprotonated product. The identities of peaks are presented in Table 3.

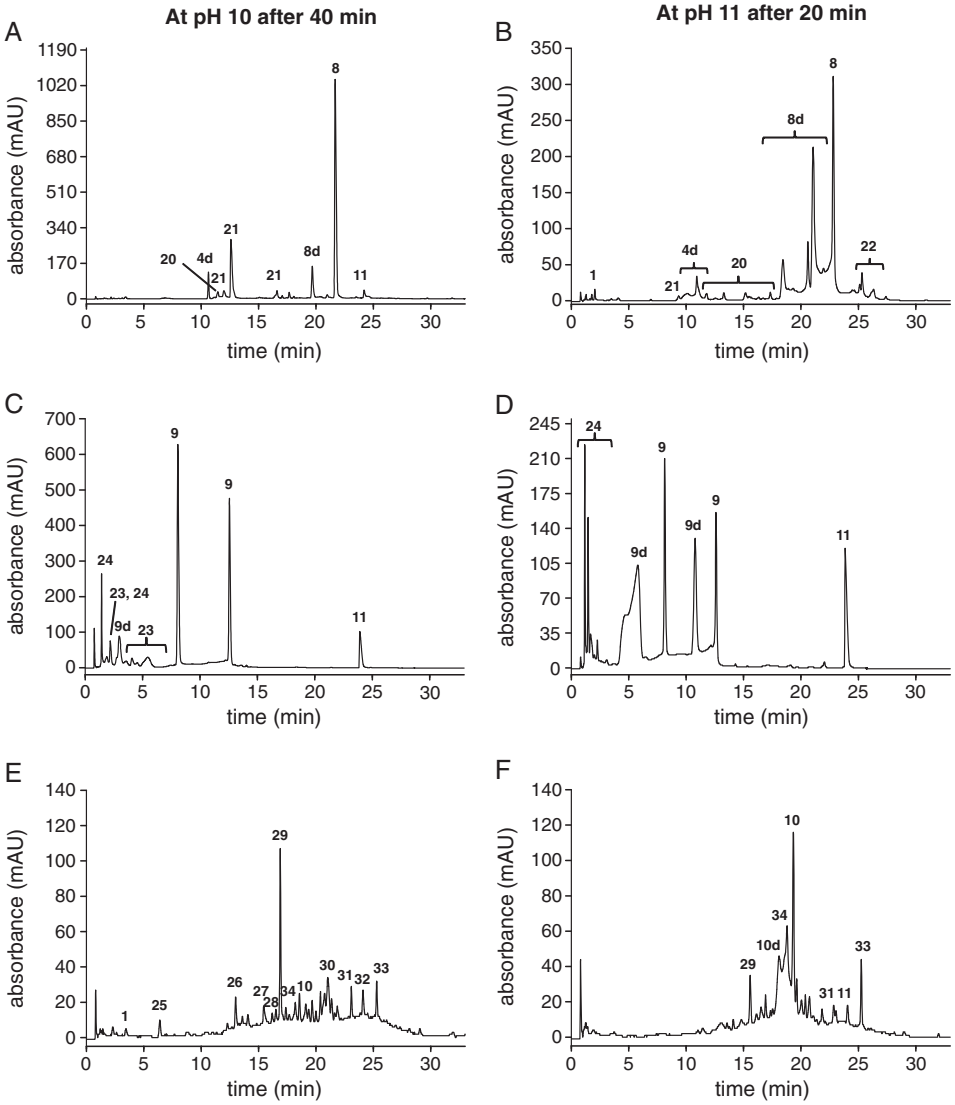

Figure 6. Comparison of HPLC chromatograms with detection wavelength 280 nm of ellagitannins at pH 10 after incubation for 40 min, and at pH 11 after incubation for 20 min. (A) Ellagitannin **8** at pH 10; (B) ellagitannin **8** at pH 11; (C) pedunculagin (**9**) at pH 10; (D) pedunculagin at pH 11; (E) geraniin (**10**) at pH 10; (F) geraniin at pH 11. The letter d indicates the deprotonated product. The identities of peaks are presented in Table 3.

similar manner (Fig. 8B and C). These products of all HTs are best explained with different pK_a values of phenolic hydroxyls depending on their position. On average, pK_a values of phenolic hydroxyl groups of gallic acid have been between 8.7 and 11.5 (Beltrán *et al*., 2003). From the coupling of galloyl groups results that the pK_a values of phenolic hydroxyls of ellagic acid are near 11.0 (Hasegawa *et al*., 2003). Similarly, it seems that the coupling of HHDP groups has increased the pK_a values of hydroxyl groups in such a way that some hydroxyls are not deprotonated until at pH 11. When the pH increased above the pK_a value of phenolic hydroxyl groups, the peaks of deprotonated HTs became more pronounced in addition to the hydrolysis products in the HPLC chromatograms and yielded the fast reaction rate of HTs at pH 10 and 11 (Figs 4 and 8 and Table 2).

The observed phenolate ions can oxidise to semiquinones when, for example, oxygen molecules quench an additional electron from ionised oxygen. When another electron is quenched in sequence, quinones can be produced (Fig. 1; Appel, 1993). All HTs were colourless in their initial solutions. During incubation, reaction solutions turned yellow at pH 9 and above. However, compounds **3**, **5** and all ETs **8–10** first turned reddish at pH 10 and 11 for ten min and then turned to yellow. This was most evident with the usual HHDP ETs. The red colour of the solution can indicate that *ortho*-quinone structures were formed first. The extracted chromatogram at 500 nm showed that two products of ellagitannin **8** and four of ellagitannin **9** had UV spectra exhibiting a third maximum in the red colour region, indicating the presence of quinone in the structure (Fig. 7A and B). One of these is product **22**, which has a third maximum at 492 nm (Table 3 and Fig. 6A and B). Those products containing quinone were seen only at pH 10 and were mainly decayed before 20 min. Quinones easily react further and form products that are here categorised to oxidatively transformed products.

Oxidatively transformed products. The third class contains miscellaneous products that had mainly higher molecular masses than the initial compounds. Ellagitannins **8** and **9** were susceptible to oxidative reactions that transformed the structure

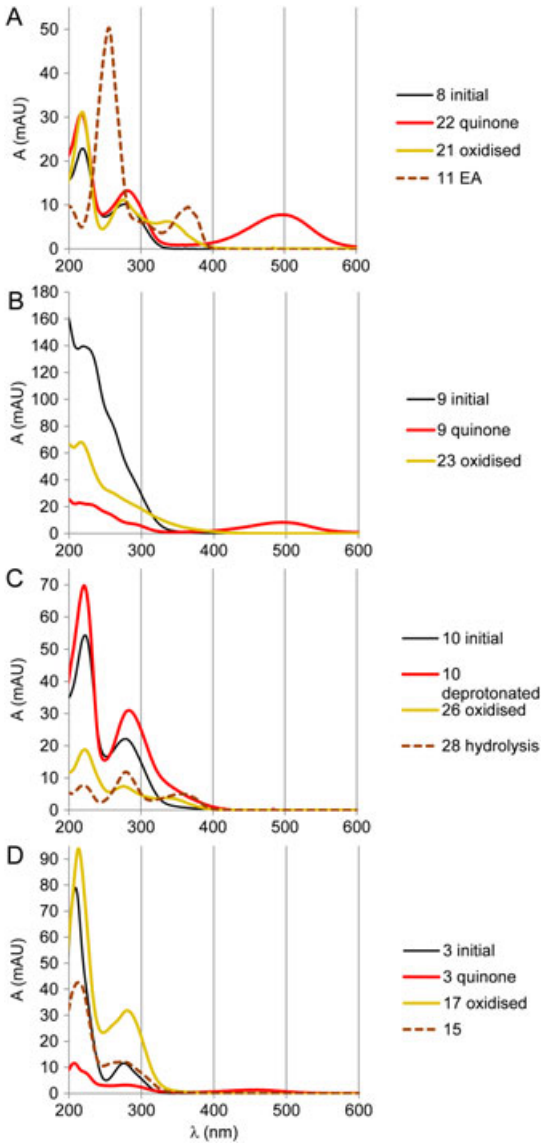

Figure 7. UV spectra for some initial compounds and their degradation products. (A) Ellagitannin **8**; (B) pedunculagin (**9**); (C) geraniin (**10**) and (D) epigallocatechin gallate (**3**).

especially at pH 10 (Fig. 6A and C). These ETs bearing HHDP groups formed several products, **21** and **23**, with molecular masses that indicated the addition of two oxygen atoms (+32 Da) to the initial structures (Fig. 6A and C and Table 3). It is proposed that these products are formed when quinones, which were detected at first, are oxidised further to acids as shown in Fig. 3. These both exhibited a doubly charged fragment ion corresponding to the cleavage of 118 Da (Table 3), which can be composed of the simultaneous cleavage of the acid group –COOH (45 Da) and the –C=OCOOH group (73 Da) from the proposed structure (Fig. 3). These oxidation products had similar UV spectra to the initial compounds except that the second UV maximum had a slowly descending shoulder (**23** in Fig. 7B) or a relatively clear third maximum near the yellow region at 350 nm (**21** in Fig. 7A). These oxidation products were not stable and degraded fast after exhibiting a maximum concentration at 20 min (such as **23** in Fig. 8E).

The dehydrohexahydroxydiphenoyl (DHHDP) group of geraniin is already an oxidised form of the HHDP group that has further dehydrated, as presented in Fig. 3. Geraniin (**10**) degraded fast and produced a complex mixture of transformed products **25–34** (Fig. 6E and F and Table 3). Many of these products exhibited an $[M-COOH]^-$ ion in their mass spectra, which indicated that they contained carboxyl groups (Table 3). Previously it has been reported that the DHHDP group of geraniin transforms to the dehydrochebuloyl group as in repandusidic acid (**34**) (structure presented in Fig. 3) or to the brevifolin carboxyl group under a brief treatment with basic aqueous solutions (Tanaka *et al*., 1990; Tanaka, 2009). The 3,6-HHDP group of **10** (Fig. 3) can undergo a similar oxidation pathway to other ETs **8** and **9**, which leads to products such as **26** and **27**, of which cleavage of even four acid groups is possible as the mass spectral fragmentation indicated (Table 3). These two products had a quite clear third UV maximum near 340 nm (Table 3). This can indicate that the ester bond also might been cleaved because the UV spectra of these products resembled that of brevifolin carboxylic acid (**28**), which is a known hydrolysis product of geraniin (Fig. 7C). A strongly simplified mechanism for this oxidation pathway is presented in Fig. 3. Okuda *et al*. (2009) and Yoshida *et al*. (2009) have reviewed the exact mechanism of the oxidation of the HHDP group and all structural variations that can be formed.

Interestingly, oxidation reactions of epigallocatechin gallate (**3**) were very similar to reactions of galloyl derivatives and ETs. Epigallocatechin gallate formed dimeric products **13–17** (Table 3 and Fig. 5C) through coupling from pyrogalloyl B rings (Tanaka, 2009). The proposed structures for the main products and oxidation pathway are presented in Fig. 2. These types of products are called theasinensins and are formed in tea during enzymatic fermentation and in mild neutral solutions at room temperature (Hatano *et al*., 2004; Tanaka, 2009). The molecular mass of product **14** corresponded to a simple dimeric structure where the B rings of epigallocatechin moieties are coupled similarly to the galloyls in the HHDP groups of ETs (Fig. 2). Product **16** had also a dimeric structure and its molecular mass fits well to the loss of H_2 and formaldehyde (−30 Da) from the molecular mass of **14** and these data can indicate product structure similar to theasinensin P-2 (Neilson *et al*., 2007). This product reached a higher concentration than the other products of **3** after 20 min and it was still present in the solution after 1 h. After that, its concentration began to slowly decrease. Formation of these kinds of relatively stable dimeric oxidation products might explain the greater ability of **3** to yield reactive oxygen species, especially H_2O_2 (Elbling *et al*., 2005; Neilson *et al*., 2007).

The formation of ellagic acid

It was a surprising result that monogalloyl derivatives also formed so much EA because traditionally it has been thought that it can only be formed from ETs after hydrolysis. Therefore, the main hydrolysis product EA was individually quantified. All HTs studied formed EA, although the amount of produced EA and the time needed to reach the maximum concentration varied greatly (Table 2). At mildly basic pH 9 and 8, the maximum formation of EA was not reached during reaction monitoring (Table 2 and Fig. 8). At pH 3, a small amount of EA was also observed.

Table 3. Examples of reaction products and initial hydrolysable tannins for reference

No.	Identification	Product type	R_t (min)	UV_{max} (nm)	Molecular composition	*m/z* values	Reference
1	MonoG glucose		3.7	217, 276	$C_{13}H_{16}O_{10}$	331.07 $[M-H]^-$, 663.14 $[2M-H]^-$	
2	MonoG quinic acid	Hydrolysis of **5**	7.5	217, 276	$C_{14}H_6O_{10}$	343.07 $[M-H]^-$, 687.14 $[2M-H]^-$, 169.02 $[GA-H]^-$, 191.06 $[QA-H]^-$, 325.06 $[M-H_2O-H]^-$	
3	EGCG		19.4	207, 275	$C_{22}H_{18}O_{11}$	457.08 $[M-H]^-$, 915.16 $[2M-H]^-$, 305.07 $[M-G-H]^-$	
4	DiG glucose	Hydrolysis of **7**	15.9	218, 277	$C_{20}H_{20}O_{14}$	483.07 $[M-H]^-$, 967.15 $[2M-H]^-$, 241.03 $[M-2H]^{2-}$, 331.06 $[M-G-H]^-$	
5	DiG quinic acid		15.7	218, 276	$C_{21}H_{20}O_{14}$	495.08 $[M-H]^-$, 991.16 $[2M-H]^-$, 343.07 $[M-G-H]^-$, 325.06 $[M-G-H_2O-H]^-$	
6	DiG glucitol		22.6	217, 276	$C_{20}H_{20}O_{13}$	467.08 $[M-H]^-$, 935.17 $[2M-H]^-$, 233.04 $[M-2H]^{2-}$, 315.07 $[M-G-H]^-$	
7	PentaG glucose		29.5	218, 280	$C_{41}H_{32}O_{26}$	939.11 $[M-H]^-$, 469.05 $[M-2H]^{2-}$, 1409.67 $[2M-H]^-$, 769.09 $[M-GA-H]^-$	
8	DiG-4,6-HHDP-glucose		21.9	218, 277	$C_{34}H_{26}O_{22}$	785.08 $[M-H]^-$, 300.99 $[EA-H]^-$, 392.04 $[M-2H]^{2-}$, 615.06 $[M-GA-H]^-$, 169.02 $[GA-H]^-$	
9	Pedunculagin		8.1/12.6	200, 227	$C_{34}H_{24}O_{22}$	783.07 $[M-H]^-$, 1567.14 $[2M-H]^-$, 391.03 $[M-2H]^{2-}$	
10	Geraniin		19.3	221, 278	$C_{41}H_{28}O_{27}$	951.07 $[M-H]^-$, 466.03 $[M-2H]^{2-}$, 300.99 $[EA-H]^-$, 633.07 $[M-318-H]^-$	
11	EA	Hydrolysis of all	24.2	252, 367	$C_{14}H_6O_8$	300.99 $[M-H]^-$, 603.01 $[2M-H]^-$	
12	MonoG glucitol	Hydrolysis of **6**	10.2/11.0	218, 276	$C_{13}H_{16}O_9$	315.07 $[M-H]^-$	
13	EGCG-MOx-D2	Dimeric of **3**	17.1	208, 275	$C_{44}H_{34}O_{24}$	945.13 $[M-H]^-$, 450.07 $[M-COOH-H]^{2-}$, 901.14 $[M-COOH]^-$, 374.07 $[M-COOH-G-H]^{2-}$	Hatano *et al.*, 2004
14	Theasinensin	Dimeric of **3**	21.1	208, 275	$C_{44}H_{34}O_{22}$	913.15 $[M-H]^-$, 456.07 $[M-2H]^{2-}$, 380.06 $[M-G-2H]^{2-}$, 591.11	Tanaka, 2009
15	Unknown	Of **3**	23.4	208, 272[a]	$C_{25}H_{18}O_{13}$	525.07 $[M-H]^-$, 355.05 $[M-GA-H]^-$	
16	Theasinensin P-2	Dimeric of **3**	24.8	207, 275	$C_{43}H_{32}O_{21}$	883.14 $[M-H]^-$, 713.12 $[M-GA-H]^-$, 497.07, 327.05, 301.00	Neilson *et al.*, 2007
17	Theasinensin quinone	Dimeric of **3**	31.0	222, 275[a]	$C_{44}H_{32}O_{22}$	911.13 $[M-H]^-$, 455.06 $[M-2H]^{2-}$, 1367.70 $[3M-2H]^{2-}$, 379.06 $[M-G-2H]^{2-}$	
18	TriG glucose	Hydrolysis of **7**	16.8	217, 280	$C_{27}H_{24}O_{18}$	635.09 $[M-H]^-$	
19	TetraG glucose	Hydrolysis of **7**	23.3	218, 280	$C_{34}H_{28}O_{22}$	787.10 $[M-H]$–, 393.05 $[M-2H]^{2-}$, 1181.66 $[3M-2H]^{2-}$, 617.08 $[M-GA-H]^-$	
20	MonoG-HHDP-glucose	Hydrolysis of **8**	11.5	219, 276	$C_{27}H_{22}O_{18}$	633.07 $[M-H]^-$, 316.03 $[M-2H]^{2-}$	

Table 3. *(Continued)*

No.	Identification	Product type	R_t (min)	UV_{max} (nm)	Molecular composition	*m/z* values	Reference
21	ET (−2H; +2OH$^-$)	Adduct/oxidation of **8**	12.7	218, 274, 337	$C_{34}H_{26}O_{24}$	817.07 [M − H]–, 531.07 [M − GA − 118]$^-$, 350.04 [M − 118]$^{2-}$, 408.03 [M − 2H]$^{2-}$,	
22	ET quinone (−2H)	Oxidation of **8**	25.5	217, 281, 492	$C_{34}H_{24}O_{22}$	783.07 [M − H]$^-$, 300.99 [EA − H]$^-$, 587.07 [M + H_2O − COOH − GA]$^-$, 378.04 [M + H_2O − COOH]$^{2-}$	
23	ET (−2H; +2OH$^-$)	Adduct/oxidation of **9**	2.0, 5.4	220[a]	$C_{34}H_{24}O_{24}$	815.06 [M − H]$^-$, 349.04 [M − 118]$^{2-}$	
24	HHDP-glucose	Hydrolysis of **9**	1.5, 2.4	197, 230	$C_{20}H_{18}O_{14}$	481.06 [M − H]$^-$, 963.13 [2M − H]$^-$, 349.04 [M − 132 − H]$^-$, 300.99 [EA − H]$^-$	
25	ET	Hydrolysis/oxidation of **10**	6.5	223, 280	$C_{34}H_{20}O_{16}$	683.07 [M − H]$^-$, 350.99 [M − 332 − H]$^-$, 537.09 [M − 145 − H]$^-$	
26	ET (−2H; +4OH$^-$)	Oxidation of **10**	13.1	221, 276, 336	$C_{41}H_{30}O_{31}$	1017.06 [M − H]$^-$, 508.03 [M − 2H]$^{2-}$, 261.00, 332.99	
27	ET (−3H; +3OH$^-$)	Oxidation of **10**	15.5	216, 277, 353	$C_{41}H_{28}O_{30}$	999.06 [M − H]$^-$, 410.04 [M − 4COOH]$^{2-}$, 261.00, 332.99	
28	Brevifolin carboxylic acid	Hydrolysis of **10**	16.3	222, 278, 354	$C_{13}H_8O_8$	291.01 [M − H]$^-$, 247.02 [M − COOH]$^-$	
29	ET (+2OH$^-$)	Oxidation of **10**	17.0	224, 276	$C_{41}H_{30}O_{29}$	985.08 [M − H]$^-$, 439.04 [M − 2COOH − H_2O]$^{2-}$, 492.03 [M − 2H]$^{2-}$	
30	ET (+O)	Oxidation of **10**	21.4	221, 280	$C_{41}H_{28}O_{28}$	967.07 [M − H]$^-$, 483.03 [M − 2H]$^{2-}$, 461.03 [M − COOH − H]$^{2-}$, 635.09 [M − 332 − H]$^-$, 327.14	
31	ET (+H_2O)	Oxidation of **10**	23.1	223, 278	$C_{41}H_{30}O_{28}$	969.08 [M − H]$^-$, 484.03 [M − 2H]$^{2-}$, 925.09 [M − COOH]$^-$, 462.04 [M − COOH − H]$^{2-}$	
32	ET quinone (−2H)	Oxidation of **10**	25.3	224, 277	$C_{41}H_{26}O_{27}$	949.06 [M − H]$^-$, 438.03 [M − 2H]$^{2-}$, 300.99 [EA − H]$^-$	
33	ET (geraniinic acid type)	Oxidation of **10**	18.6/25.3	219, 278	$C_{41}H_{28}O_{27}$	951.07 [M − H]$^-$, 453.04 [M − COOH − H]$^{2-}$, 475.03 [M − 2H]$^{2-}$	
34	ET (+H_2O; repandusidic acid)	Oxidation of **10**	18.9	220, 276	$C_{41}H_{30}O_{28}$	969.08 [M − H]$^-$, 633.07 [M− 336 − H]$^-$, 462.04 [M − COOH − H]$^{2-}$, 247.02 [Brevifolin − H]$^-$	Tanaka *et al.*, 1990

G, galloyl; GA, gallic acid; EA, ellagic acid; QA, quinic acid; EGCG, epigallocatechin gallate.
[a]Slowly descending shoulder.

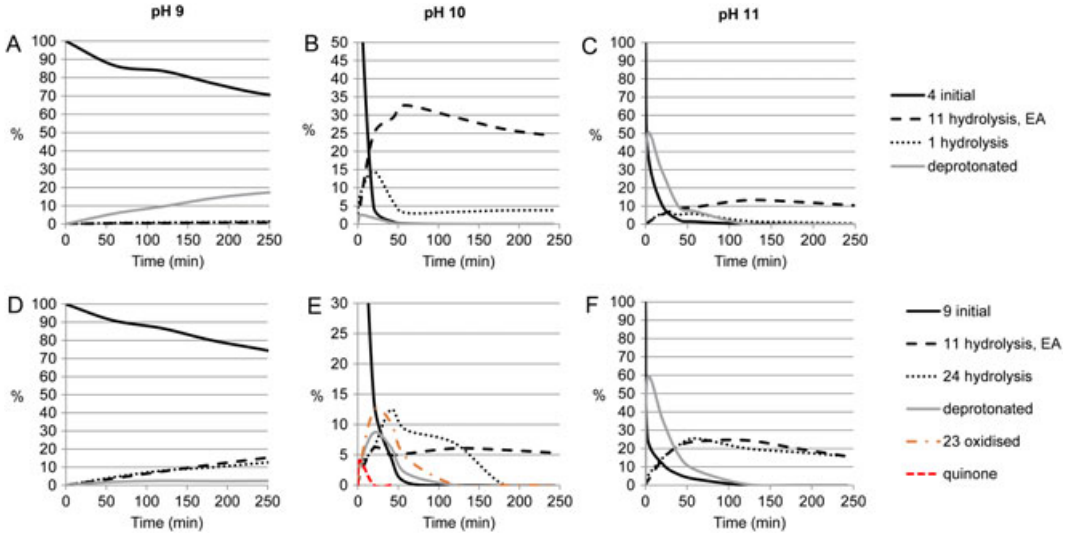

Figure 8. Relative formation of degradation products compared with the peak area of the initial compound at 280 nm in a time-scale. Data points are average values of three replicates. (A) Digalloyl glucose (**4**) at pH 9; (B) digalloyl glucose at pH 10; (C) digalloyl glucose at pH 11; (D) pedunculagin (**9**) at pH 9; (E) pedunculagin at pH 10; (F) pedunculagin at pH 11. The compound numbers refer to Table 3.

The formation of EA from **3** was the slowest for all the compounds studied. This result was an expected because EGCG (**3**) does not really belong to HTs, although it contains the same gallate moiety. The decreasing amount of **3** was explained by the formation of other types of products observed (Table 3) instead of hydrolysis products. Based on the formation of EA, the susceptibility to hydrolysis among different polyols decreased in the following order: glucose > glucitol > quinic acid (Table 2).

When the maximum formed amount of EA is compared with the calculated maximum (Table 2), which includes all galloyl and HHDP groups of the initial structure, it is clear that all groups are not equally susceptible to hydrolysis. MonoGG (**1**) forms the highest relative amount of EA although it reached only 60.8% of the calculated maximum concentration (Table 2). Even the pentaGG that formed the highest total amount of EA seemed to readily hydrolyse only one or two galloyl groups (Table 2 and Fig. 5D). Usually galloyl groups have a more facile hydrolytic cleavage than HHDP groups because fewer bonds have to break. Although galloyl groups are hydrolysed more easily in acidic conditions, whereas HHDP groups are hydrolysed more easily in basic conditions (Hemingway and Hillis, 1971).

Ellagitannin **9** was the only exception that formed more EA at pH 11 than at pH 10 and it also formed EA at pH 9, whereas all other HTs did not hydrolyse efficiently at that pH. This indicates that the other HHDP group is more easily hydrolysed in mildly basic pH than galloyl groups. The other HHDP group is more resistant to hydrolysis because hydrolysis product **24** containing one HHDP was still present after 4 h even at pH 11 (Fig. 8F). Typically the 2,3-HHDP group is more resistant to hydrolysis than 4,6-HHDP (Yoshida *et al*., 1992). Geraniin was more persistent to hydrolysis than ETs **8** and **9**. However, small amounts of hydrolysis products **20** and **1** were observed and thus DHHDP seemed to be the most easily cleaved group from geraniin (**10**). Moreover, a small amount of brevifolin carboxylic acid (**28**) was detected, which is the lactonised product of the hydrolysed DHHDP group (Fig. 6E).

Interestingly, the maximum concentrations of EA increased with the amount of galloyl groups, but not with the amount of HHDP groups (Table 2), although ellagic acid is considered to be the hydrolysis product of ETs. The formation of EA from gallic acid, pentaGG or similar compounds without the HHDP groups has been encountered occasionally in alkaline conditions (Yoshida *et al*., 1989) or with the strong oxidant peroxidase (Kamel *et al*., 1977; Fig. 1). It seems that hydrolysed and deprotonated galloyl groups are not stable alone in alkaline solutions and thus dimerisation and lactonisation to ellagic acid happens fast (Fig. 1). Similar coupling happened with EGCG (Fig. 2). Li *et al*. (2007) have stated that oxidative coupling between two pyrogalloyl B-rings is the major oxidation route.

Ellagic acid was the main product left after incubation of several hours and is thus relatively stable in basic conditions. However, its amount began to slowly decrease after the maximum was reached (Fig. 8) and degradation products with similar UV spectra and *m/z* at 303 were detected. The mass of this product indicates that one lactone bond might have opened, which has also been observed to occur above pH 9 and leads to the greenish brown colour (Bala *et al*., 2006). The contents of EA in biological studies might have been underestimated because of its poor water-solubility. It might have been precipitated and filtered away from neutral or acidic sample solutions. The approach used in this study, where sample solutions were analysed without neutralising, enabled the detection and quantification of EA from an aqueous solution.

Summary

It was observed that the browning and yellow colour observed in the pro-oxidant measurements might be a result of several reaction products. The fast colour change of samples to yellow can be due to the deprotonation of the phenolic hydroxyls groups because ionisation shifts the UV maxima to longer wavelengths. Slower increase in colour can result from the slower formation of other oxidatively transformed products and hydrolysis products such as ellagic acid. It can be concluded that pH level is a strong determinant in the fate of tannins, and HPLC/DAD combined with high-resolution ESI/QTOF/MS is an efficient method for the identification of various reaction products.

Acknowledgements

This work was funded by grants from the Emil Aaltonen Foundation and Turku University Foundation (to AT). The authors wish to thank Jaana Liimatainen, Olli Martiskainen and Jari Sinkkonen for their assistance with the MS and NMR measurements. Juha-Pekka Salminen, Johanna Moilanen, Maarit Karonen and Jari Sinkkonen helped to improve the earlier version of the manuscript.

References

Appel HM. 1993. Phenolics in ecological interactions: The importance of oxidation. *J Chem Ecol* **19**: 1521–1552.

Appel HM, Martin MM. 1990. Gut redox conditions in herbivorous Lepidopteran larvae. *J Chem Ecol* **16**: 3277–3290.

Bala I, Bhardwaj V, Hariharan S, Ravi Kumar MNV. 2006. Analytical methods for assay of ellagic acid and its solubility studies. *J Pharm Biomed Anal* **40**: 206–210.

Barbehenn RV, Constabel PC. 2011. Tannins in plant–herbivore interactions. *Phytochemistry* **72**: 1551–1565.

Barbehenn RV, Jones CP, Hagerman AE, Karonen M, Salminen JP. 2006. Ellagitannins have greater oxidative activities than condensed tannins and galloyl glucoses at high pH: potential impact on caterpillars. *J Chem Ecol* **32**: 2253–2267.

Barbehenn RV, Weir Q, Salminen JP. 2008. Oxidation of ingested phenolics in the tree-feeding caterpillar *Orgyia leucostigma* depends on foliar chemical composition. *J Chem Ecol* **34**: 748–756.

Barbehenn RV, Jaros A, Lee G, Mozola C, Weir Q, Salminen JP. 2009. Hydrolyzable tannins as 'quantitative defenses': Limited impact against *Lymantria dispar* caterpillars on hybrid poplar. *J Insect Physiol* **55**: 297–304.

Barbehenn RV, Niewiadomski J, Kochmanski J. 2012. Limited effect of reactive oxygen species on the composition of susceptible essential amino acids in the midguts of *Lymantria dispar* caterpillars. *Arch Insect Biochem Physiol* **81**: 160–177.

Beltrán JL, Sanli N, Fonrodona G, Barrón D, Özkan G, Barbosa J. 2003. Spectrophotometric, potentiometric and chromatographic pK_a values of polyphenolic acids in water and acetonitrile–water media. *Anal Chim Acta* **484**: 253–264.

Davis AL, Cai Y, Davies AP, Lewis JR. 1996. ^{1}H and ^{13}C NMR assignments of some green tea polyphenols. *Magn Res Chem* **34**: 887–890.

Elbling L, Weiss RM, Teufelhofer O, Uhl M, Knasmueller S, Schulte-Hermann R, Berger W, Micksche M. 2005. Green tea extract and (−)-epigallocatechin-3-gallate, the major tea catechin, exert oxidant but lack antioxidant activities. *FASEB J* **19**: 807–809.

Gross EM, Brune A, Walenciak O. 2008. Gut pH, redox conditions and oxygen levels in an aquatic caterpillar: Potential effects on the fate of ingested tannins. *J Insect Physiol* **54**: 462–471.

Haddock EA, Gupta RK, Haslam E. 1982. The metabolism of gallic acid and hexahydroxydiphenic acid in plants. Part 3.[1] Esters of (*R*)- and (*S*)-hexahydroxydophenic acid and dehydrohexahydroxydiphenic acid with □-glucopyranose ($^{1}C_4$ and related conformations). *J Chem Soc Perkin Trans I* **11**: 2535–2545.

Hasegawa M, Terauchi M, Kikuchi Y, Nakao A, Okubo J, Yoshinaga T, Hiratsuka H, Kobayashi M, Hoshi T. 2003. Deprotonation processes of ellagic acid in solution and solid states. *Monat Chem* **134**: 811–821.

Hatano T, Hattori S, Ikeda Y, Shindu T, Okuda T. 1990. Gallotannins having a 1,5-anhydro-D-glucitol core and some ellagitannins from *Acer* species. *Chem Pharm Bull* **37**: 1902–1905.

Hatano T, Hori M, Kusuda M, Ohyabu T, Ito H, Yoshida T. 2004. Characterization of the oxidation products of (−)-epigallocatechin gallate, a bioactive tea polyphenol, on incubation in neutral solution. *Heterocycles* **63**: 1547–1554.

Hemingway RW, Hillis WE. 1971. Behaviour of ellagitannins, gallic acid, and ellagic acid under alkaline conditions. *Tappi* **54**: 933–936.

Johnson KS, Barbehenn RV. 2000. Oxygen levels in the gut lumens of herbivorous insects. *J Insect Physiol* **46**: 897–903.

Kamel MY, Saleh NA, Ghazy AM. 1977. Gallic acid oxidation by turnip peroxidase. *Phytochemistry* **16**: 521–524.

Li Y, Tanaka T, Kouno I. 2007. Oxidative coupling of the pyrogalloyl B-ring with a galloyl group during enzymatic oxidation of epigallocatechin 3-O-gallate. *Phytochemistry* **68**: 1081–1088.

Moilanen J, Salminen JP. 2008. Ecologically neglected tannins and their biologically relevant activity: chemical structure of plant ellagitannins reveal their in vitro oxidative activity at high pH. *Chemoecology* **18**: 73–83.

Neilson AP, Hopf AS, Cooper BR, Pereira MA, Bomser JA, Ferruzzi MG. 2007. Catechin degradation with concurrent formation of homo- and heterocatechin dimers during *in vitro* digestion. *J Agric Food Chem* **55**: 8941–8949.

Nishimura H, Nonaka G, Nishioka I. 1984. Seven quinic acid gallates from *Quercus stenophylla*. *Phytochemistry* **23**: 2621–2623.

Okuda T, Yoshida T, Hatano T, Ito H. 2009. Ellagitannins renewed the concept of tannins. In *Chemistry and Biology of Ellagitannins, an Underestimated Class of Bioactive Plant Polyphenols*. Quideau S (ed.). World Scientific: Singapore; 1–54.

Saijo R, Nonaka GI, Nishioka I. 1990. Gallic acid esters of bergenin and nonbergenin from *Mallotus japonicus*. *Phytochemistry* **29**: 267–270.

Salminen JP, Karonen M. 2011. Chemical ecology of tannins and other phenolics: we need a change in approach. *Funct Ecol* **25**: 325–338.

Salminen JP, Ossipov V, Haukioja E, Pihlaja K. 2001. Seasonal variation in the content of hydrolysable tannins in leaves of *Betula pubescens*. *Phytochemistry* **57**: 12–22.

Tanaka T. 2009. Physicochemical properties and biomimetic reactions of ellagitannins. In *Chemistry and Biology of Ellagitannins, an Underestimated Class of Bioactive Plant Polyphenols*. Quideau S (ed.). World Scientific: Singapore; 119–151.

Tanaka T, Nonaka G-I, Nishioka I. 1990. Tannins and related compounds. C.1) Reaction of dehydrohexahydroxydiphenic acid esters with bases, and its application to the structure determination of pomegranate tannins, granatins A and B. *Chem Pharm Bull* **38**: 2424–2428.

Tanaka T, Kirihara S, Nonaka G-I, Nishioka I. 1993. Tannins and related compounds. CXXIV.1) Five new ellagitannins, platycaryanins A, B, C and D, and platycariin, and a new complex tannin, strobilanin, from the fruits and bark of *Platycarya strobilacea* SIEB *et* ZUCC., and biomimetic synthesis of *C*-glycosidic ellagitannins from glucopyranose-based ellagitannins. *Chem Pharm Bull* **41**: 1708–1716.

Winkler LW. 1888. Die Bestimmung des in Wasser Gelösten Sauerstoffes. *Berichte der Deutschen Chmeischen Gesellschaft* **21**: 2843–2855.

Yagi K, Goto K, Nanjo F. 2009. Identification of a major polyphenol and polyphenolic composition in leaves of *Camellia irrawadiensis*. *Chem Pharm Bull* **57**: 1284–1288.

Yoshida T, Mori K, Hatano T, Okumura T, Uehara I, Komagoe K, Yuzaburo F, Okuda T. 1989. Studies on inhibition mechanism of autoxidation by tannins and flavonoids. V.1) Radical-scavenging effects of tannins and related polyphenols on 1,1-diphenyl-2-picrylhydrazyl radical. *Chem Pharm Bull* **37**: 1919–1921.

Yoshida T, Hatano T, Kuwajima T, Okuda T. 1992. Oligomeric hydrolysable tannins – their ^{1}H NMR spectra and partial degradation. *Heterocycles* **33**: 463–482.

Yoshida T, Hatano T, Ito H, Okuda T. 2009. Structural diversity and antimicrobial activities of ellagitannins. In *Chemistry and Biology of Ellagitannins, an Underestimated Class of Bioactive Plant Polyphenols*. Quideau S (ed.). World Scientific: Singapore; 55–93.